

Human exposure to respiratory aerosols in a ventilated room: Effects of ventilation condition, emission mode, and social distancing

Gen Pei, Mary Taylor, Donghyun Rim *

Department of Architectural Engineering, Pennsylvania State University, United States



ARTICLE INFO

Keywords:

Airborne infection
COVID-19
Indoor airflow
Social distance
Eulerian-Eulerian model
Computational Fluid Dynamics (CFD)

ABSTRACT

Airborne transmission of virus via respiratory aerosols plays an important role in the spread of infectious diseases in indoor environments. Ventilation and social distancing are two major control strategies to reduce the indoor airborne infection risk. However, there is a present lack of science-based information on how the human exposure to viral aerosols vary with ventilation condition and social distance. The objective of this study is to explore the transport patterns of respiratory aerosols in occupied spaces and assess the occupant exposure risk under different ventilation strategies, social distances and aerosol emission modes. The study results show that buoyancy-driven flow regime (can be found in many residential settings) can lead to a longer transmission distance and elevated exposure to viral aerosols than the mixing airflow, thereby causing higher cross-infection risk in indoor environments. The results also suggest that a 2 m (6 ft) social distance alone may not ensure control of indoor airborne infections.

1. Introduction

The novel coronavirus (SARS-CoV-2) pandemic threatens global public health and human well-being. The SARS-CoV-2 is known to be transmitted through large respiratory droplets ($>5\text{--}10 \mu\text{m}$) from infected individuals during breathing, talking, coughing, and sneezing (WHO World Health Organization, 2020; CDC, 2020; Chan et al., 2020; Ghinai et al., 2020; Luo et al., 2020; Pung et al., 2020). Evidence has also indicated that the airborne transmission of small exhaled droplets ($<5 \mu\text{m}$), is an important contributor to the spread of the disease (Balachandar, Zaleski, Soldati, Ahmadi, & Bourouiba, 2020; Bourouiba, 2020; Fennelly, 2020; Ge et al., 2020; Guo et al., 2020; Jin et al., 2021; Liu et al., 2020; Morawska & Cao, 2020; Santarpia et al., 2020; Setti et al., 2020; Van Doremalen et al., 2020). Compared to the larger droplets, the small, virus-laden aerosols can accumulate in indoor air for hours and travel a longer distance carried by the indoor airflow (Bourouiba, 2020; Guo et al., 2020; Morawska & Cao, 2020; Setti et al., 2020; Van Doremalen et al., 2020). Van Doremalen (2020) reported that the SARS-CoV-2 can remain viable in airborne particles for 3 h allowing it time to spread within a space. Guo et al. (2020) collected air in an intensive care unit and detected air samples positive for SARS-CoV-2 at 14 of the 40 sampling sites. Their results showed that the transmission distance of SARS-CoV-2 aerosols can be up to 4 m. A study by Bourouiba

(2020) revealed that the infectious aerosols generated by sneezing can reach a distance of 7–8 m. Morawska and Cao (2020) highlighted that small aerosols may carry the virus over a distance of tens of meters. Furthermore, in indoor environments (e.g., buildings and cruise ships) operating with air recirculation systems, the airborne particles can be transported to different rooms through the air distribution systems and facilitate the spread of airborne infection (Morawska and Cao, 2020; Ong et al., 2020; Elias & Bar-Yam, 2020; Almilaji & Thomas, 2020). Furthermore, the sub-micron aerosols can deposit in the lower respiratory tract of a human which leads to a more severe infection (Brown, Cook, Ney, & Hatch, 1950; Fennelly, 2020; Tellier, Li, Cowling, & Tang, 2019). As people spend most of their time in indoor environments ($>20 \text{ h}$ daily, even longer time during the pandemic) (Klepeis et al., 2001), reducing human exposure to viral aerosols in occupied spaces is a key step towards controlling the spread of the disease among population.

Social distancing and ventilation are two widely recognized control strategies to reduce the airborne infection risk in indoor environments (WHO World Health Organization, 2020; CDC, 2020; ASHRAE, 2020; REHVA, 2020). The World Health Organization (WHO World Health Organization, 2020) and US Centers for Disease Control and Prevention (CDC, 2020) have recommended maintaining an inter-personal social distance larger than 1–2 m. In addition to keeping a social distance, studies have emphasized the importance of sufficient ventilation in

* Corresponding author at: 222 Engineering Unit A, University Park, PA, 16802, United States.

E-mail addresses: gup33@psu.edu (G. Pei), dxr51@psu.edu (D. Rim).

mitigating the airborne disease transmission. Chen and Zhao (2020) pointed out that insufficient ventilation found in makeshift hospitals could increase airborne transmission of SARS-CoV-2. Buonanno, Stabile, and Morawska (2020) found that an increase in the air change rate from 0.2 h^{-1} to 2.2 h^{-1} in a pharmacy can reduce the reproduction number (R_0) of SARS-CoV-2 from 2.34 to 0.80. Other studies have also demonstrated the association between inadequate ventilation and increased infection risk of COVID-19 as well as other airborne infectious diseases (Morawska & Milton, 2020; Somsen, van Rijn, Kooij, Bem, & Bonn, 2020; Stadnytskyi, Bax, Bax, & Anfinrud, 2020; CDC, 2005; Li et al., 2007; Myatt et al., 2004; Morawska et al., 2020).

Besides the amount of ventilation air, the indoor airflow pattern associated with ventilation strategy can affect the spatial distribution of viral aerosols and hence the occupant exposure risk (Bhagat, Wykes, Dalziel, & Linden, 2020; Guo et al., 2021; Li, Huang, Yu, Wong, & Qian, 2005; Lu et al., 2020; Nielsen, Li, Buus, & Winther, 2010; Qian et al., 2006; Rim & Novoselac, 2010a, 2009; Villafruela, Castro, San José, & Saint-Martin, 2013). Lu et al. (2020) observed that the airflow from an air conditioner prompted a COVID-19 infection event in a restaurant due to an inappropriate supply air direction. Experiments by Qian et al. (2006) showed that human exposure to exhaled aerosols in a hospital ward with displacement ventilation can be 29 % higher than that with mixing ventilation, and can be 39 % higher than the case with downward ventilation. Rim and Novoselac (2010a, 2009) illustrated the impacts of near-human airflow characteristics on the breathing zone concentration of airborne particles. Several other studies reported that with poorly-designed airflow patterns, increasing the ventilation rate may lead to even higher airborne infection risk (Bolashikov, Melikov, Kierat, Popiolek, & Brand, 2012; Melikov, Bolashikov, Kostadinov, Kierat, & Popiolek, 2012; Pantelic & Tham, 2013).

There have been debates about what ventilation strategy and social distancing requirement are effective to control airborne disease transmission in indoor environments (Setti et al., 2020; Sun & Zhai, 2020). Clearly, advanced knowledge of human exposure risk to respiratory aerosols under various indoor airflow patterns is needed when determining effective ventilation system and social distancing protocol. However, there is a present lack of science-based information on how the aerosol transport varies near the occupant breathing zone depending on the airflow pattern, social distance and aerosol emission mode (e.g., talking vs. breathing). Given this background, the objective of the present study is to fill this knowledge gap by examining (1) the transport dynamics of respiratory aerosols in occupied spaces under representative indoor ventilation strategies: mixing ventilation and displacement ventilation; and (2) how human exposure risk varies with ventilation condition, social distance and aerosol emission mode. This research can

provide useful information that helps building designers and policy-makers to improve decision-making of what ventilation scheme and social distance are effective to control airborne infectious diseases in different indoor environments.

2. Method

This study investigated transport of respiratory aerosols from an infector in a ventilated room based on the Eulerian-Eulerian multi-phase model using Computational Fluid Dynamics (CFD) simulations. Using this model, we also evaluated the application of tracer gas as a proxy of small (sub-micron) aerosols and conducted a parametric analysis to investigate the efficacy of ventilation strategy and social distancing on reducing airborne infection risk.

2.1. Model geometry and boundary conditions

The baseline model simulated transport of respiratory aerosols from an infector's talking in a displacement ventilated room, as shown in Fig. 1a. Displacement ventilation creates a buoyancy-driven airflow regime through low-momentum supply air at the floor level. Note that residential rooms without mechanical fan operating often exhibit buoyancy-driven airflow patterns similar to displacement ventilation (Rim & Novoselac, 2009). The modeled room was a typical residential room or small office with dimensions of 4 m (length) \times 4 m (width) \times 3.63 m (height). Two face-to-face detailed geometries of sedentary humans (Sørensen & Voigt, 2003) with a distance of 1 m (nose to nose) were simulated. A social distance > 1 m is recommended by WHO (2020) to reduce the airborne disease transmission. The heat load produced by each human (53 W/m^2) was divided into convective and radiative loads at 45 % and 55 %, respectively, based on the literature (Gao & Niu, 2004; Sørensen & Voigt, 2003). The convective heat was applied to the human surface as a Neumann thermal boundary condition and the radiative portion was evenly distributed to the surrounding wall surfaces (Shan & Rim, 2018). The supply air flow rate was $36 \text{ m}^3/\text{h}$ (equivalent to air change rate $= 0.6 \text{ h}^{-1}$) based on the minimum ventilation requirements as defined by ANSI/ASHRAE (2019). The supply air was set as 100 % outdoor air at a supply temperature of 17°C (ASHRAE, 2019).

Releases of particles (density = 1000 kg/m^3) via an exhalation jet flow from the mouth of the infector were simulated for aerosol emission due to talking (see Fig. 1a). Based on the literature, the exhaled airspeed due to talking was set as 4 m/s (Chao et al., 2009; Kwon et al., 2012) and the temperature of the exhaled air was 34°C (Ai & Melikov, 2018). The area of mouth was set as 1.15 cm^2 and the exhalation jet was released in

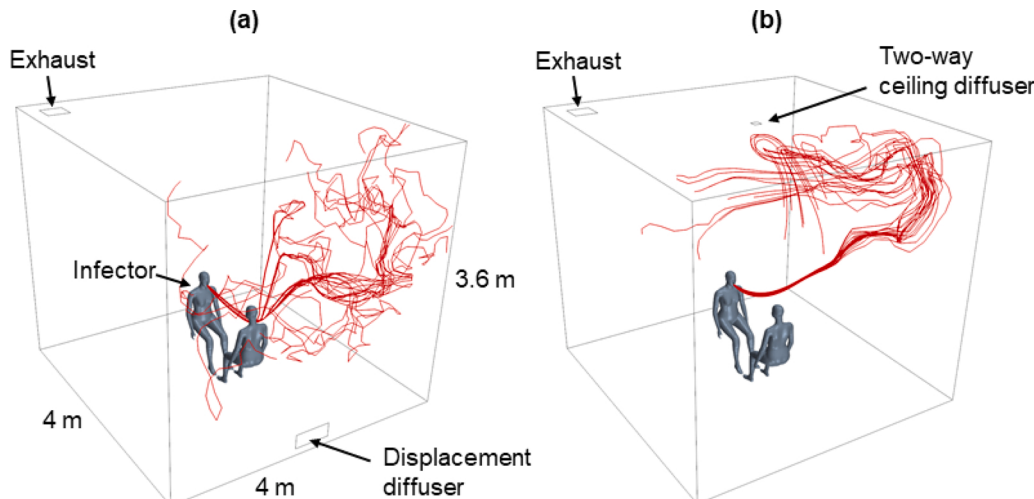


Fig. 1. Streamlines of exhaled airflow in an occupied room with (a) displacement ventilation and (b) mixing ventilation.

a horizontal direction (Ai & Melikov, 2018). Two aerosol sizes of 1 μm and 10 μm were simulated given that 0.1–10 μm is the dominant size range of the respiratory aerosols (Ai & Melikov, 2018). The aerosol concentration of the infector's breath was set to 1 $\mu\text{g}/\text{m}^3$, by which the aerosol concentrations in the room were normalized. In this study, aerosol deposition was considered only for the floor surface as previous studies reported that the deposition velocity of particles larger than 1 μm at the floor is 1–3 magnitudes higher than that at the sidewall and ceiling (Lai & Nazaroff, 2000; Rim & Novoselac, 2010b). According to the results of Lai and Nazaroff (2000), the deposition velocity at the floor was set as 0.003 cm/s for 1 μm aerosols, and 0.3 cm/s for 10 μm aerosols based on the airflow conditions of the present study.

2.2. Eulerian-Eulerian particle model

The Eulerian two-fluid model (also known as the Eulerian-Eulerian model) was employed to predict the transport of the airborne aerosols. The Eulerian-Eulerian model solves two sets of conservation equations for two phases (i.e., airflow and particles) and incorporates the interactions between two phases including drag force, lift force, and turbulent dispersion force (Li, Yan, Shang, & Tu, 2015; Yan, Li, & Ito, 2020). This modeling approach has been previously used to predict particle transport in indoor environments and it shows comparable accuracy with the Lagrangian model and better performance than the drift-flux model (Li et al., 2015; Yan et al., 2020). In addition, the Eulerian-Eulerian model can directly obtain the particle concentration while saving the computational cost compared to the Lagrangian model. For the modeling of flow turbulence, the Reynolds Averaged Navier-Stokes approach with a Shear Stress Transport $k-\omega$ model was adopted due to its good performance in simulating the stratified airflow associated with buoyance-driven plumes near humans (Gilani, Montazeri, & Blocken, 2016; Menter, 1994; Pei, Rim, Schiavon, & Vannucci, 2019).

2.3. Mesh generation and model verification

Polyhedral mesh was used to construct the computational grids given its flexibility for detailed human geometry and its potential to reduce computational cost while maintaining reasonable accuracy (Peric & Ferguson, 2005). The meshes were refined in the proximity of the human body to improve the accuracy for modeling the exhalation jet and aerosol transport near the body (see Fig. 2). The first cell size adjacent to the human surface was 5 mm with a cell stretch rate of 1.3, corresponding to an average y^+ value (i.e., dimensionless wall distance) at the human surface of 3.5 (Pei & Rim, 2021). The meshes near

grid-sensitive regions such as the supply air inlet and outlet were also refined. A total of 140,000 cells were generated for the simulation domain.

To ensure consistent simulation results with mesh refinements, the grid sensitivity analysis was performed by observing the influence of the grid resolution on the predicted aerosol concentration within the human breathing zone of the exposed occupant (a 500 cm^3 cuboid below the nose tip). Three grid resolutions: 60,000, 140,000 (adopted in this study), and 180,000 cells, were tested. Table S1 in Supporting Information provides detailed parameters of these three grid resolutions. Fig. S1 shows that the discrepancy in simulated breathing zone aerosol concentration is less than 3 % for the grid refinement from 140,000 cells to 180,000 cells, suggesting that the mesh used in this study (140,000 cells) can produce converged solution of the particle transport near the occupant breathing zone with reasonable accuracy.

In addition to the grid sensitivity test, the CFD model results were verified by comparing the simulated aerosol concentration at the room exhaust with the well-mixed mass balance model as follows (Nazaroff & Cass, 1986; Rim & Novoselac, 2008):

$$C_{ex} = \frac{G}{(\lambda + \beta)V}(1 - e^{-(\lambda + \beta)t}) \quad (1)$$

where C_{ex} is the exhaust aerosol concentration, G is the aerosol emission rate, λ is the air change rate, β is the aerosol deposition rate ($\beta = \frac{v_d A}{V}$, v_d is the deposition velocity, A is the deposition surface area and V is the room volume), and t is the time.

2.4. Parametric analysis

The Eulerian-Eulerian particle model was compared further with a tracer gas model. Previous studies have shown the potential of using a tracer gas as a proxy to simulate the transport of small aerosols (< 3.5 μm) in indoor environments (Qian et al., 2006; Pantelic and Tham., 2013; Ai & Melikov, 2018; Rim & Novoselac, 2008; Zhang, Chen, Mazumdar, Zhang, & Chen, 2009; Noakes et al., 2009; Beato Arribas, McDonagh, Noakes, & Sleigh, 2015; Bivolarova, Ondráček, Melikov, & Ždímal, 2017). In this study, the tracer gas model shared the same computational grids and airflow simulation parameters as the Eulerian-Eulerian model. The dispersion of an inert gas (i.e., sulfur hexafluoride, SF₆) was simulated by solving a three-dimensional convection-diffusion mass transfer equation (Ferziger, Perić, & Street, 2002).

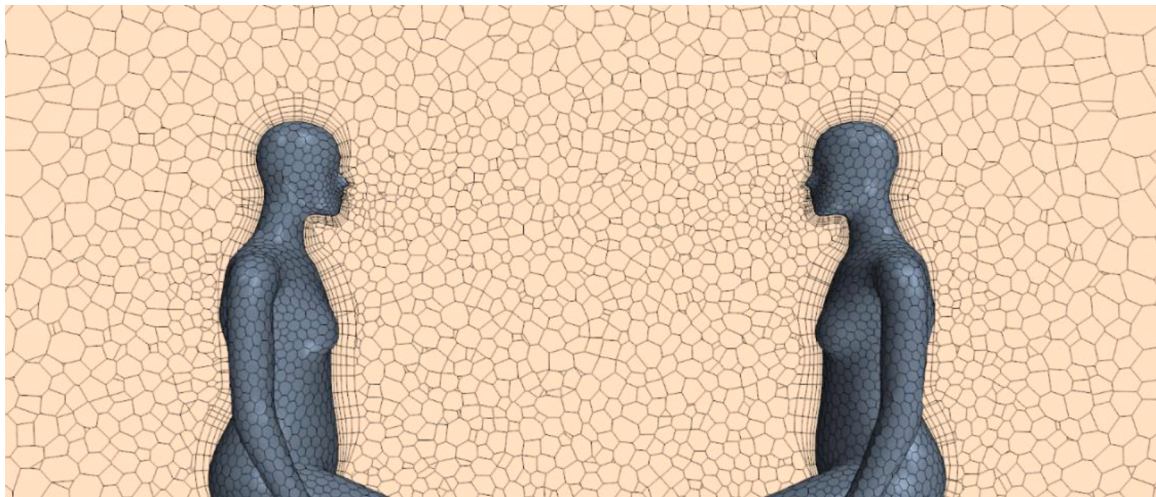


Fig. 2. Details of the computational grids near the human bodies.

$$\frac{\partial(\rho C)}{\partial t} + \nabla \cdot (\rho C \mathbf{u}) = \nabla \cdot (D_{\text{eff}} \nabla C) + S_c \quad (2)$$

where ρ is the density of fluid, C is the tracer gas concentration, t is the time, \mathbf{u} is the fluid velocity vector, D_{eff} is the effective diffusion coefficient including molecular diffusion and turbulent diffusion, and S_c is the source or sink term.

After confirming the capability of the tracer gas model to predict the transport of small respiratory aerosols (details in Section 3.1), we then carried out the parametric analysis using the tracer gas model to evaluate the impacts of ventilation strategy (displacement ventilation vs. mixing ventilation), air change rate (0.6 h^{-1} vs. 3 h^{-1}), social distance (1 m vs. 2 m), and aerosol emission mode (talking vs. breathing), as summarized in Table 1. The boundary conditions for the model of displacement ventilation were provided in Section 2.1. For the mixing ventilation model, 100 % outdoor air was introduced through a high-momentum two-way ceiling diffuser at the center of the ceiling (see Fig. 1b). The supply airspeed was set at 2.15 m/s with the air temperature of 17°C and the supply air direction angled at 25° from the ceiling plane (Awwad, Mohamed, & Fatouh, 2017). Compared to the displacement ventilation, the mixing ventilation introduces a high-momentum supply airflow to the room that can facilitate room air mixing (Ahn, Rim, & Lo, 2018). Note that the ventilation rate of 0.6 h^{-1} is based on the minimum ventilation rate recommended by ANSI/ASHRAE Standard 62.1 (2019), while the ventilation rate of 3.0 h^{-1} represents indoor spaces with mechanical ventilation systems such as a variable air volume system or a dedicated outdoor air system (ANSI/ASHRAE, 2019).

Regarding the aerosol emission process, besides the aerosol emission mode of talking (described in Section 2.1), the aerosol emission from normal breathing was also investigated. According to the literature, the aerosols with an exhalation jet were constantly emitted in a horizontal direction from the mouth (mouth area = 1.15 cm^2) of the infector (Ai & Melikov, 2018). The exhalation air speed due to breathing was set as 1.5 m/s with the air temperature of 34°C (Ai & Melikov, 2018). Note that this study set a constant exhalation and did not model the inhalation process based on that the inhaled concentration can be measured with accuracy less than 5% without the simulation of breathing cycle if the sampling location is $<0.01 \text{ m}$ from the upper lip (Melikov & Kaczmarczyk, 2007). Furthermore, these assumptions were adopted in previous experimental and CFD studies that examined the transport of exhaled aerosols, which reported that these assumptions can provide reasonable insight into the human exposure to exhaled aerosols (Gao & Niu, 2004; Li, Niu, & Gao, 2011; Li, Niu, & Gao, 2013; Zhu, Kato, & Yang, 2006; Yan, Zhang, Sun, & Li, 2009; Yin, Gupta, Zhang, Liu, & Chen, 2011).

To evaluate the risk of cross-infection under different ventilation and social distancing conditions, the time-varying aerosol concentration within the human breathing zone of the exposed occupant was monitored for each simulation (Rim, Novoselec, & Morrison, 2009). Furthermore, intake fraction (iF), a widely used exposure risk

assessment method, was employed to assess the inhalation infection risk (Ai & Melikov, 2018; Licina, Tian, & Nazaroff, 2017; Nazaroff, 2008). Intake fraction (iF) is defined as the ratio of inhaled pollutant mass by the exposed occupant (M_{inhale}) to the exhaled pollutant mass from the infector (M_{exhale}):

$$iF = \frac{M_{\text{inhale}}}{M_{\text{exhale}}} = \frac{\int_0^T Q_b C_{bz}(t) dt}{\int_0^T E(t) dt} \quad (3)$$

where $Q_b = 0.6 \text{ m}^3/\text{h}$ is the breathing flow rate for an individual at rest (Ai & Melikov, 2018), $C_{bz}(t)$ is the aerosol concentration in the exposed occupant's breathing zone, $E(t)$ is the aerosol emission rate (which is constant in this study), and T is the aerosol emission time. To verify the application of intake fraction, the predicted intake fraction by the simulation of mixing ventilation was compared with the analytical solution for well-mixed condition (Nazaroff, 2008), and the discrepancy was less than 0.8 % for the simulation time of 60 min.

3. Results and discussion

3.1. Transport of respiratory aerosols and evaluation of tracer gas model

Fig. 3 compares the time-varying concentration contours of the tracer gas, $1 \mu\text{m}$ aerosols, and $10 \mu\text{m}$ aerosols associated with the infector's talking under displacement ventilation with an air change rate of 0.6 h^{-1} . The distance between the occupants (nose to nose) is 1 m. Note that the concentrations are normalized by the emission concentration. The figure shows that all three types of the pollutants (i.e., tracer gas, $1 \mu\text{m}$ aerosols, and $10 \mu\text{m}$ aerosols) can penetrate into the exposed occupant's breathing zone (the region below the nose tip) within 1 min carried by the exhalation jet from talking. These results indicate that a 1 m social distance is not adequate to prevent the human exposure to exhaled aerosols in this case. Furthermore, these pollutants can accumulate in the breathing zone over time. This pattern is attributed to the influence of the exhalation jet from talking on the thermal plume around the exposed occupant (Gao & Niu, 2006). Under displacement ventilation, the buoyancy-driven thermal plumes are formed near the occupants due to the temperature gradient between the human body and the ambient room air (see the airflow and temperature fields in Fig. S2). The thermal plumes with relatively high vertical airspeeds have the potential to move the viral aerosols away from the breathing zone to the upper region of the room (Pei et al., 2019; Rim & Novoselec, 2009). However, the study results herein show that the high-momentum exhalation jet from talking can penetrate into the exposed occupant's thermal plume and increase the human exposure to exhaled aerosols (see Fig. 3). Note that this pattern can also be observed in residential rooms without mechanical air mixing that exhibit buoyancy-driven airflow regime.

The comparisons between the tracer gas and the $1 \mu\text{m}$ aerosols in their concentration contours (Fig. 3) suggest that tracer gas has spatial transport patterns fairly similar to the $1 \mu\text{m}$ aerosols. The $10 \mu\text{m}$ aerosols also exhibit similar distribution patterns at the early stages of the

Table 1

Summary of the simulation cases and key results. Note that the concentrations are normalized by the emission concentration. DV: displacement ventilation. MV: mixing ventilation.

Case	Species	Social distance (m)	Ventilation strategy	Air change rate (h^{-1})	Aerosol emission mode	Human breathing zone concentration ($\times 10^{-2}$)			Intake fraction ($\times 10^{-3}$)	
						1 min	10 min	60 min	10 min	60 min
1	1 μm aerosol	1	DV	0.6	Talking	3.15	3.47	4.66	12.2	15.0
2	10 μm aerosol	1	DV	0.6	Talking	3.02	3.40	3.92	11.9	13.8
3	Tracer gas	1	DV	0.6	Talking	3.04	3.34	4.89	11.7	15.1
4	Tracer gas	2	DV	0.6	Talking	2.15	2.49	4.08	8.32	11.9
5	Tracer gas	1	DV	0.6	Breathing	0.30	0.51	1.07	1.90	11.4
6	Tracer gas	1	DV	3	Talking	0.014	0.132	0.340	0.235	0.932
7	Tracer gas	1	MV	0.6	Talking	0.0002	0.423	2.09	0.712	4.29

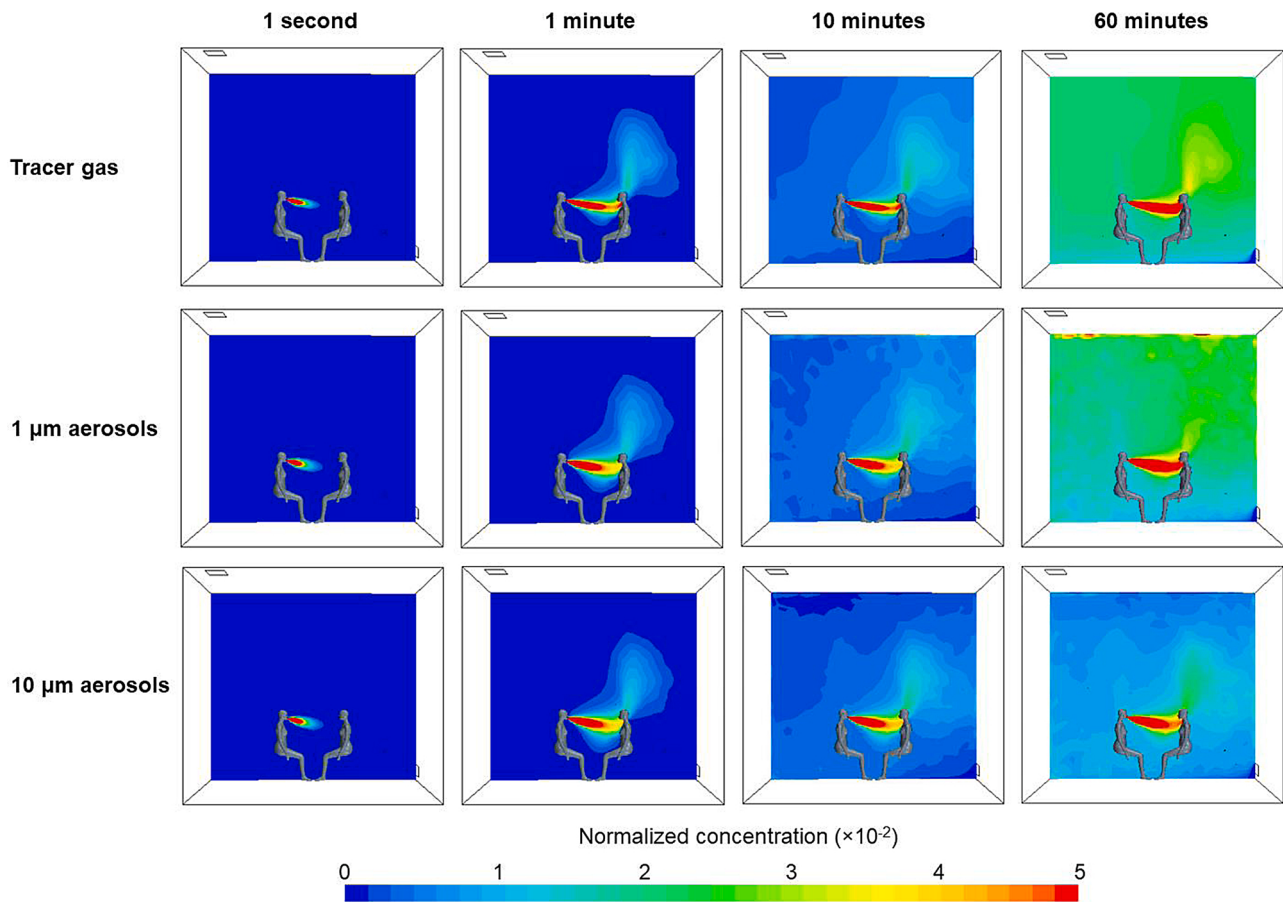


Fig. 3. Temporal concentration development of the tracer gas, 1 μm aerosols, and 10 μm aerosols under displacement ventilation with an air change rate of 0.6 h^{-1} . The social distance is 1 m and the aerosol emission mode is talking. Note that the concentrations are normalized by the emission concentration.

simulation (<10 min); however, at 60 min, the room concentration pattern of 10 μm aerosols is notably different from that of the tracer gas. This discrepancy is mainly due to the higher deposition rate of the 10 μm aerosols that results in much lower concentrations than 1 μm aerosols. More quantitative comparisons are discussed below.

Fig. 4 compares the transient concentration profiles of the tracer gas, 1 μm aerosols, and 10 μm aerosols. Note that for each subfigure, four different concentration profiles are presented: 1) Human breathing zone concentration represents the volume-averaged concentration within a 500 cm^3 cuboid below the nose tip of the exposed occupant; 2) ASHRAE breathing zone concentration is defined as the volume-averaged

concentration in the region from 7.55 cm to 180 cm above the floor and further than 60 cm from the walls (ANSI/ASHRAE, 2019); 3) Exhaust concentration is the area-averaged concentration of the room exhaust based on the CFD simulation; and 4) Theoretical solution represents the concentration calculated using the well-mixed mass balance model (see Eq. 1). For all of the three pollutants, the concentration in the human breathing zone of the exposed occupant rapidly increases in a short time (<1 min). The human breathing zone concentration is remarkably higher than the room exhaust concentration and the ASHRAE breathing zone concentration, implying that the exhaust concentration and ASHRAE breathing zone concentration cannot accurately reflect actual

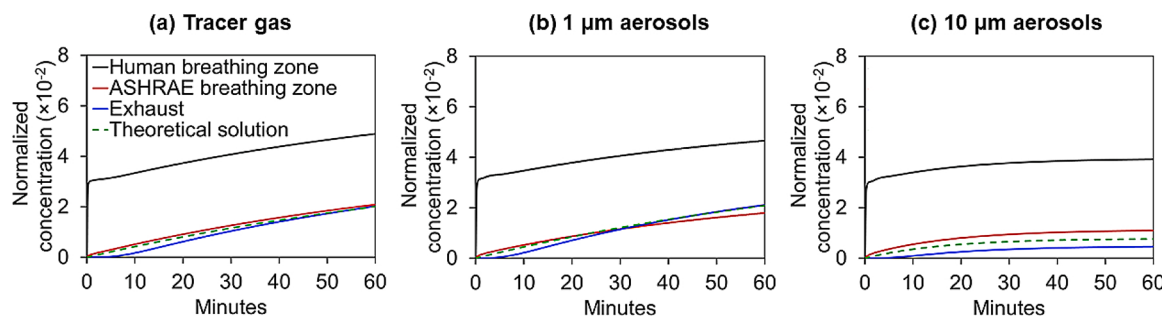


Fig. 4. Transient concentration profiles of (a) tracer gas, (b) 1 μm aerosols and (c) 10 μm aerosols under displacement ventilation at an air change rate of 0.6 h^{-1} . The social distance is 1 m and the aerosol emission mode is talking. The human breathing zone concentration represents the volume-averaged concentration within a 500 cm^3 cuboid below the nose tip of the exposed occupant. The ASHRAE breathing zone concentration is defined as the volume-averaged concentration in the region from 7.55 cm to 180 cm above the floor and further than 60 cm from the walls. The exhaust concentration is the area-averaged concentration of the room exhaust based on the CFD simulation. The theoretical solution represents the concentration calculated using the well-mixed mass balance model. Note that the concentrations are normalized by the emission concentration.

human exposure under displacement ventilation. For the $1\text{ }\mu\text{m}$ aerosols, the human breathing zone concentration is >120 % higher than the exhaust concentration and >160 % larger than the ASHRAE breathing zone concentration. This high aerosol concentration in the human breathing zone reveals that a 1 m social distance is not sufficient to reduce exposure to viral aerosols emitted from talking under displacement ventilation. Furthermore, Fig. 4 illustrates that theoretical room concentration computed by the well-mixed model can largely underestimate the human exposure.

The comparisons between Fig. 4a and b suggest that the tracer gas model can serve as a proxy to predict the human exposure to $1\text{ }\mu\text{m}$ aerosols. The difference between the tracer gas and the $1\text{ }\mu\text{m}$ aerosols in the human breathing zone concentration is smaller than 5%. Furthermore, the tracer gas model can predict the intake fraction of $1\text{ }\mu\text{m}$ aerosols with a discrepancy as 4% at 10 min and 0.7 % at 60 min (see Table 1). Note that the Eulerian-Eulerian model of $1\text{ }\mu\text{m}$ aerosols requires approximately five times the computing time of the tracer gas simulation. For the prediction of the human breathing zone concentration of the $10\text{ }\mu\text{m}$ aerosols, the tracer gas model can provide reasonable results with discrepancies <3 % for the initial 10 min, whereas the discrepancy increases to 25 % at 60 min.

Fig. 4b and c show that the influence of aerosol size (< $10\text{ }\mu\text{m}$) on the human exposure is not pronounced at the early stages of the simulation. For example, at 10 min, the difference in human breathing zone concentration between $1\text{ }\mu\text{m}$ and $10\text{ }\mu\text{m}$ aerosols is only 2 %, and the difference in intake fraction is 3 % (see Table 1). This trend is mainly because the exhalation jet dominates the aerosol transport and the aerosol deposition loss is relatively small during the early period of

emission (<10 min). However, at 60 min, the difference in human breathing zone concentration between two aerosol sizes increases up to 16 %.

3.2. Efficacy of social distancing

After confirming the capability of the tracer gas model in predicting the human exposure to small respiratory aerosols, we proceed to use the tracer gas model to analyze the efficacy of social distancing. Fig. 5a and b depict the tracer gas concentration contours after a 1 min talking with a 1 m and 2 m social distance, and Fig. 5c and d present the transient concentration profiles for two social distances. It is observed that even with a 2 m social distance, the emitted pollutants from talking can still travel to the exposed occupant's breathing zone within 1 min (Fig. 5b). Accordingly, the pollutant concentration in the human breathing zone rapidly elevates within 1 min with the level more than twice the average room concentration (Fig. 5d). These results reveal that the viral aerosols released from talking can travel a 2 m distance in a short time in indoor environments under a buoyancy-driven flow regime. In such cases, social distancing alone may not be an effective control strategy to mitigate the airborne disease infections.

Fig. S3 presents the transport pattern of tracer gas associated with normal breathing. Compared to talking, the exhalation jet from breathing penetrates a shorter distance due to the smaller initial exhaled airspeed, which leads to a lower human exposure to the exhaled pollutants. The human breathing zone concentration of pollutants due to breathing is 85 % lower than that from talking at 10 min (see Table 1). It should be noted that this reduction in human exposure for the case with

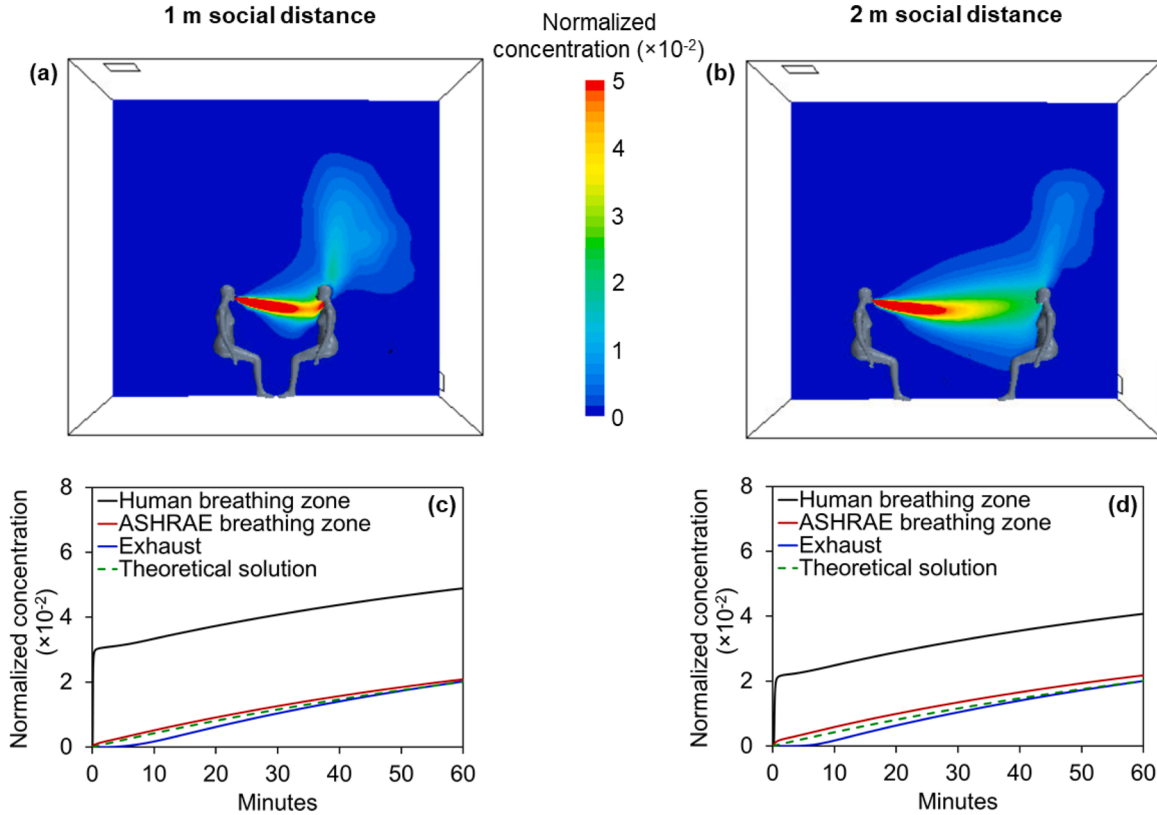


Fig. 5. Figs. (a) and (b) are the contours of tracer gas concentration at a simulation time of 1 min with a social distance of 1 m and 2 m. Figs. (c) and (d) are the transient concentration profiles of tracer gas with a social distance of 1 m and 2 m. The ventilation system is displacement ventilation with an air change rate of 0.6 h^{-1} . The aerosol emission mode is talking. The human breathing zone concentration represents the volume-averaged concentration within a 500 cm^3 cuboid below the nose tip of the exposed occupant. The ASHRAE breathing zone concentration is defined as the volume-averaged concentration in the region from 7.55 cm to 180 cm above the floor and further than 60 cm from the walls. The exhaust concentration is the area-averaged concentration of the room exhaust based on the CFD simulation. The theoretical solution represents the concentration calculated using the well-mixed mass balance model. Note that the concentrations are normalized by the emission concentration.

breathing is not only caused by the smaller pollutant emission rate (62 % less than talking), but also due to the shorter exhalation jet. The intake fraction associated with breathing is 84 % smaller than that with talking at 10 min. These results suggest that different aerosol emission modes from infectors should be considered when determining effective ventilation system and safe social distancing protocol, as the emission mode can meaningfully affect the transport pattern of respiratory aerosols.

3.3. Effect of ventilation strategy

This section elucidates the impacts of ventilation strategy and air change rate on dispersion of respiratory aerosols as well as human exposure risk in indoor environments. Fig. 6 compares the tracer gas concentration distributions between displacement ventilation (DV) and mixing ventilation (MV) at an air change rate of 0.6 h^{-1} . It is observed that under MV, the exhalation jet from the infector's talking is disrupted quickly by the room airflow and travels a much shorter distance than DV, which is mainly due to the enhanced room air mixing by the high-momentum supply airflow of MV (Ahn et al., 2018). Consequently, the exhaled pollutants are relatively well-mixed with the room air and minimally accumulate in the exposed occupant's breathing zone under MV.

Fig. 7 presents the transient concentration profiles of the tracer gas under DV and MV. The figure shows that human breathing zone concentration is notably higher under DV than MV. After 10 min of talking, the human breathing zone concentration of exhaled pollutants is roughly 7 times higher for DV than MV, and the intake fraction is about 15 times higher. This is mainly because the exhalation jet travels a longer distance and the respiratory aerosols are more easily trapped in the breathing zone by the occupant thermal plume under DV than MV, as described in Fig. 6. These results suggest that with a relatively small air change rate, DV can yield poor performance in reducing the airborne infection risk compared to MV.

Fig. 7 also shows that under MV, the concentrations in the human breathing zone and at the room exhaust are fairly close due to the well-mixed condition. It appears that a 1 m social distance is good enough to prevent the rapid elevation of human exposure to exhaled aerosols from

talking under MV. In such a case, the concentrations within the ASHRAE breathing zone and at the room exhaust (both simulated and analytical) can serve as a good proxy to estimate the human exposure.

Fig. S4 depicts the concentration evolution of tracer gas under DV with an increased air change rate of 3 h^{-1} . As expected, compared to the case with a smaller air change rate of 0.6 h^{-1} (Fig. 6), the indoor pollutant concentrations are reduced because if an increased room air dilution. However, it is noteworthy that varying the ventilation flow rate can modulate the trajectory of the exhalation jet. With an air change rate of 3 h^{-1} , the thermal plume around the exposed occupant is enhanced and it can draw the exhalation jet upwards, thereby transporting the pollutants to the upper region away from the human breathing zone (see Fig. S4). Table 1 shows that increasing the air change rate from 0.6 h^{-1} to 3 h^{-1} can reduce the human breathing zone concentration by more than 90 %, and can also lower the intake fraction by 98 %. These results illustrate that increasing the ventilation rate under DV is an effective way to reduce human exposure to respiratory aerosols.

3.4. Study implications

The coronavirus outbreak (COVID-19) proposes new requirements of disease control strategies for a sustainable development of society. Ventilation and social distancing are two primary approaches to prevent the airborne virus transmission in indoor environments (WHO, 2020; CDC, 2020; Agarwal et al., 2021; Sun & Zhai, 2020). This study investigates the transport dynamics of respiratory aerosols from an infector in occupied spaces and analyzes the efficacy of ventilation strategy and social distancing on reducing the occupant exposure risk. The comparisons of simulation results between displacement ventilation (DV) and mixing ventilation (MV) show that DV yields a longer transmission distance of the exhaled aerosols from talking that causes a higher cross-infection risk than MV. This observation is consistent with a previous experimental study that reported the inhalation concentration of exhaled aerosols from normal breathing is 29 % larger under DV than MV in a two-bed hospital ward (Qian et al., 2006). The increase in inhalation concentration for DV in their study is smaller than our study (7 times higher under DV than MV) likely due to a larger air change rate

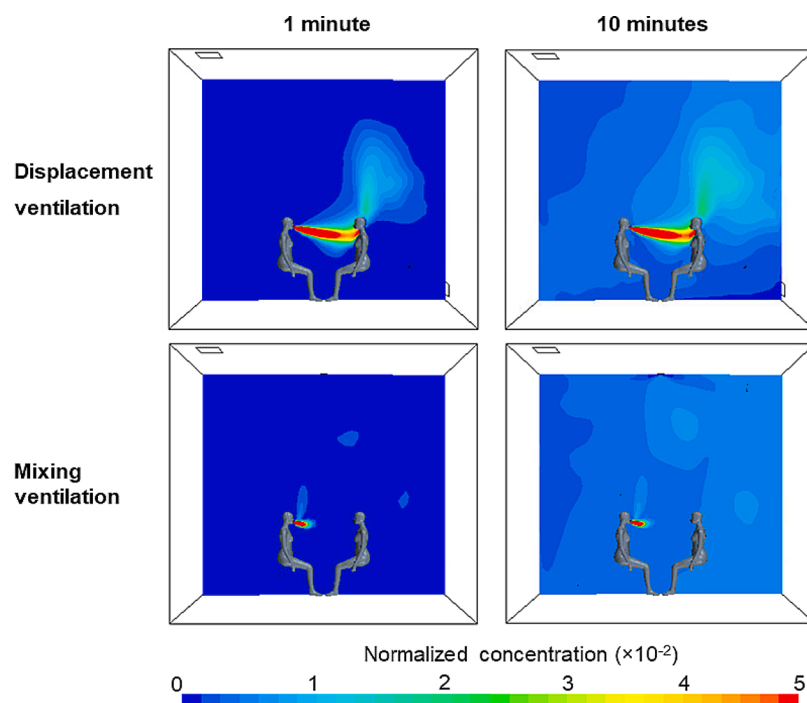


Fig. 6. Contours of tracer gas concentrations under displacement ventilation and mixing ventilation. The air change rate is 0.6 h^{-1} , the social distance is 1 m, and the aerosol emission mode is talking. Note that the concentrations are normalized by the emission concentration.

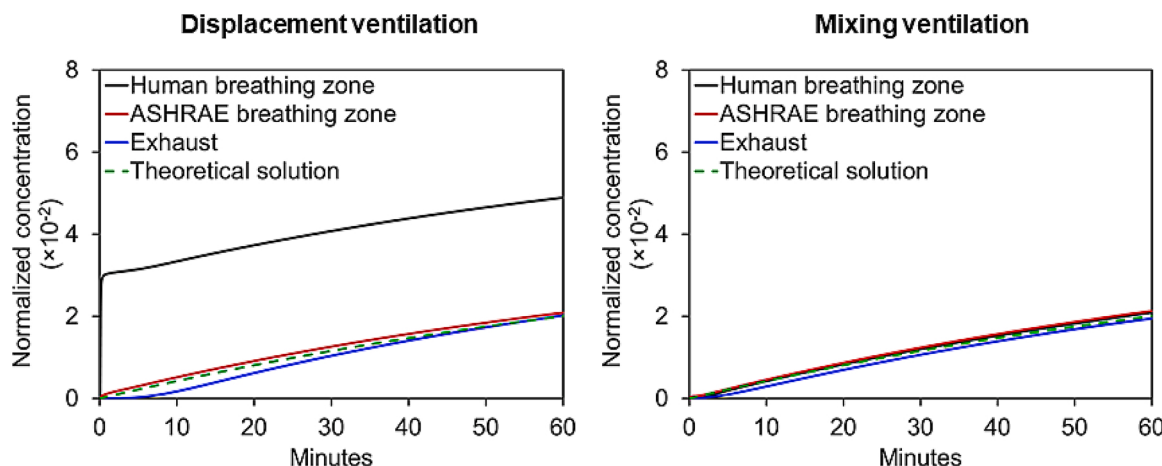


Fig. 7. Transient concentration profiles of tracer gas under displacement ventilation and mixing ventilation. The air change rate is 0.6 h^{-1} , the social distance is 1 m, and the aerosol emission mode is talking. The human breathing zone concentration represents the volume-averaged concentration within a 500 cm^3 cuboid below the nose tip of the exposed occupant. The ASHRAE breathing zone concentration is defined as the volume-averaged concentration in the region from 7.55 cm to 180 cm above the floor and further than 60 cm from the walls. The exhaust concentration is the area-averaged concentration of the room exhaust based on the CFD simulation. The theoretical solution represents the concentration calculated using the well-mixed mass balance model. Note that the concentrations are normalized by the emission concentration.

(4 h^{-1}) and a different aerosol emission mode in their study. In general, our study suggests cautions for applying DV systems in indoor environments with susceptible populations, especially in rooms with low ventilation rates.

Our study also explores the effect of social distancing on reducing the human exposure to viral aerosols. The WHO World Health Organization (2020) and many countries such as America (CDC, 2020), China (Du et al., 2020), Italy (Giordano et al., 2020), and Australia (Australian Government, 2020) have restricted a social distance of 1–2 m to control the COVID-19 pandemic. However, our study provides science-based evidence showing that a 2 m social distance alone may not ensure control of the indoor airborne infections, especially in occupied spaces with buoyancy-driven airflow regime (e.g., rooms with DV at small ventilation rates or residences without mechanical mixing fans). For the rooms with the buoyancy-driven airflow patterns, it appears that increasing ventilation rate or room air mixing is a more effective strategy than the social distancing to prevent the airborne disease transmission. In contrast, for the rooms with mixing airflows, a shorter social distance (e.g., 1 m) is good enough to mitigate the elevated human exposure to exhaled aerosols from talking. Taken together, our study suggests that control strategies for airborne disease transmission (ventilation and social distancing) should be considered together for layered controls, rather than being considered independently.

Future studies are warranted to extend the modeling and analysis approaches of this study to other building types (e.g., healthcare settings and densely occupied spaces such as classrooms) and examine effective control strategies in different indoor settings.

4. Conclusions

This study investigated the transport of respiratory aerosols from an infector in a ventilated room based on CFD simulations with the Eulerian-Eulerian model and the tracer gas model. We explored the effects of ventilation strategy, social distancing, and aerosol emission mode on human exposure to viral aerosols. The following major findings are obtained.

- 1) Tracer gas can serve as a good proxy to simulate the transport dynamics of small respiratory aerosols ($<1 \mu\text{m}$) and predict the associated human exposure risk.
- 2) 1–2 m social distances may not be sufficient to prevent the transmission of airborne aerosols ($<10 \mu\text{m}$) in indoor environments.

Specifically, in occupied spaces with buoyancy-driven airflow regime such as rooms with displacement ventilation or residential buildings without mechanical mixing fans, viral aerosols from infector's talking can travel longer than 2 m and reach the exposed occupant's breathing zone within 1 min.

- 3) Ventilation strategy meaningfully affects the human exposure to exhaled aerosols. Under displacement ventilation, the exhaled aerosols can penetrate a longer distance and lead to an elevated human exposure than mixing ventilation. The human breathing zone concentration of viral aerosols from talking can be more than 7 times higher with displacement ventilation than mixing ventilation.
- 4) Under displacement ventilation, increasing the ventilation rate can effectively reduce human exposure to respiratory aerosols mainly due to enhanced room air dilution and the change in the trajectory of the exhalation jet. An increase in the air change rate from 0.6 h^{-1} to 3 h^{-1} can achieve a more than 90 % reduction in the human breathing zone concentration for viral aerosols.
- 5) The transport pattern of respiratory aerosols and associated human exposure risk vary with the aerosol emission mode. The intake fraction of exhaled aerosols from normal breathing can be 84 % smaller than that from talking.

Declaration of Competing Interest

The authors declare that they have no known competing financial interests or personal relationships that could have appeared to influence the work reported in this paper.

Acknowledgements

The research presented in this paper was supported by the U.S. National Science Foundation (Award No. NSF Grant 2028713: RAPID: Coronavirus: Understanding aerosol transmission and potential control measures in indoor environments).

Appendix A. Supplementary data

Supplementary material related to this article can be found, in the online version, at doi:<https://doi.org/10.1016/j.scs.2021.103090>.

References

- Agarwal, N., Meena, C. S., Raj, B. P., Saini, L., Kumar, A., Gopalakrishnan, N., ... Aggarwal, V. (2021). Indoor air quality improvement in COVID-19 pandemic. *Sustainable Cities and Society*, 102942. <https://doi.org/10.1016/j.scs.2021.102942>
- Ahn, H., Rim, D., & Lo, L. J. (2018). Ventilation and energy performance of partitioned indoor spaces under mixing and displacement ventilation. In *Building simulation* (Vol. 11, pp. 561–574). Tsinghua University Press. <https://doi.org/10.1007/s12273-017-0410-z>. No. 3.
- Ai, Z. T., & Melikov, A. K. (2018). Airborne spread of respiratory droplet nuclei between the occupants of indoor environments: A review. *Indoor Air*, 28(4), 500–524. <https://doi.org/10.1111/ina.12455>
- Almilaji, O., & Thomas, P. (2020). *Air recirculation role in the infection with COVID-19, lessons learned from Diamond Princess cruise ship*. medRxiv. <https://doi.org/10.1101/2020.07.08.20148775>
- ANSI/ASHRAE. (2019). *ANSI/ASHRAE standard 62.1-2019: Ventilation for acceptable indoor air quality*. Atlanta, GA, USA: American Society of Heating, Refrigeration, and Airconditioning Engineers.
- ASHRAE. (2020). ASHRAE position document on infectious aerosols. *Refrigerating and air-conditioning engineers*. American Society of Heating.
- ASHRAE. (2019). *ASHRAE handbook: HVAC applications-chapter 58: Room air distribution*. Atlanta, GA, USA: American Society of Heating, Refrigeration, and Airconditioning Engineers.
- Australian Government, D. O. H. (2020). *Social distancing for coronavirus (COVID-19)*.
- Awwad, A., Mohamed, M. H., & Fatouh, M. (2017). Optimal design of a louver face ceiling diffuser using CFD to improve occupant's thermal comfort. *Journal of Building Engineering*, 11, 134–157. <https://doi.org/10.1016/j.jobe.2017.04.009>
- Balachandar, S., Zaleski, S., Soldati, A., Ahmadi, G., & Bourouiba, L. (2020). *Host-to-host airborne transmission as a multiphase flow problem for science-based social distance guidelines*. <https://doi.org/10.1016/j.ijmultiphaseflow.2020.103439>
- Beato Arribas, B., McDonagh, A., Noakes, C. J., & Sleigh, P. A. (2015). Assessing the near patient infection risk in isolation rooms. In *Healthy Buildings 2015-Conference Proceedings*.
- Bhagat, R. K., Wykes, M. D., Dalziel, S. B., & Linden, P. F. (2020). Effects of ventilation on the indoor spread of COVID-19. *Journal of Fluid Mechanics*, 903. <https://doi.org/10.1017/jfm.2020.720>
- Bivolarova, M., Ondráček, J., Melikov, A., & Ždímal, V. (2017). A comparison between tracer gas and aerosol particles distribution indoors: The impact of ventilation rate, interaction of airflows, and presence of objects. *Indoor Air*, 27(6), 1201–1212. <https://doi.org/10.1111/ina.12388>
- Bolashikov, Z. D., Melikov, A. K., Kierat, W., Popiółek, Z., & Brand, M. (2012). Exposure of health care workers and occupants to coughed airborne pathogens in a double-bed hospital patient room with overhead mixing ventilation. *Hvac&R Research*, 18(4), 602–615. <https://doi.org/10.1080/10789669.2012.682692>
- Bourouiba, L. (2020). Turbulent gas clouds and respiratory pathogen emissions: Potential implications for reducing transmission of COVID-19. *Jama*, 323(18), 1837–1838. <https://doi.org/10.1001/jama.2020.4756>
- Brown, J. H., Cook, K. M., Ney, F. G., & Hatch, T. (1950). Influence of particle size upon the retention of particulate matter in the human lung. *American Journal of Public Health and the Nations Health*, 40(4), 450–480. <https://doi.org/10.2105/AJPH.40.4.450>
- Buonanno, G., Stabile, L., & Morawska, L. (2020). Estimation of airborne viral emission: Quanta emission rate of SARS-CoV-2 for infection risk assessment. *Environment International*, 105794. <https://doi.org/10.1016/j.envint.2020.105794>
- CDC. (2005). *Guidelines for preventing the transmission of Mycobacterium tuberculosis in health-care settings*. US Centers for Disease Control and Prevention.
- CDC. (2020). *How COVID-19 Spreads?* US Centers for Disease Control and Prevention (Accessed January 2, 2021) <https://www.cdc.gov/coronavirus/2019-ncov/prevent-getting-sick/how-covid-spreads.html>.
- Chan, J. F. W., Yuan, S., Kok, K. H., To, K. K. W., Chu, H., Yang, J., ... Tsui, H. W. (2020). A familial cluster of pneumonia associated with the 2019 novel coronavirus indicating person-to-person transmission: A study of a family cluster. *The Lancet*, 395 (10223), 514–523. [https://doi.org/10.1016/S0140-6736\(20\)30154-9](https://doi.org/10.1016/S0140-6736(20)30154-9)
- Chao, C. Y. H., Wan, M. P., Morawska, L., Johnson, G. R., Ristovski, Z. D., Hargreaves, M., ... Katoshevski, D. (2009). Characterization of expiration air jets and droplet size distributions immediately at the mouth opening. *Journal of Aerosol Science*, 40(2), 122–133. <https://doi.org/10.1016/j.jaerosci.2008.10.003>
- Chen, C., & Zhao, B. (2020). Makeshift hospitals for COVID-19 patients: Where health-care workers and patients need sufficient ventilation for more protection. *Journal of Hospital Infection*, 105(1), 98–99. <https://doi.org/10.1016/j.jhin.2020.03.008>
- Du, Z., Xu, X., Wang, L., Fox, S. J., Cowling, B. J., Galvani, A. P., ... Meyers, L. A. (2020). Effects of proactive social distancing on COVID-19 outbreaks in 58 cities, China. *Emerging Infectious Diseases*, 26(9), 2267.
- Elias, B., & Bar-Yam, Y. (2020). *Could air filtration reduce COVID-19 severity and spread*. Cambridge, MA: New England Complex Systems Institute.
- Fennelly, K. P. (2020). Particle sizes of infectious aerosols: Implications for infection control. *The Lancet Respiratory Medicine*. [https://doi.org/10.1016/S2213-2600\(20\)30323-4](https://doi.org/10.1016/S2213-2600(20)30323-4)
- Perziger, J. H., Perić, M., & Street, R. L. (2002). *Computational methods for fluid dynamics*. Berlin: Springer.
- Gao, N., & Niú, J. (2004). CFD study on micro-environment around human body and personalized ventilation. *Building and Environment*, 39(7), 795–805. <https://doi.org/10.1016/j.buildenv.2004.01.026>
- Gao, N., & Niú, J. (2006). Transient CFD simulation of the respiration process and inter-person exposure assessment. *Building and Environment*, 41(9), 1214–1222. <https://doi.org/10.1016/j.buildenv.2005.05.014>
- Ge, X. Y., Pu, Y., Liao, C. H., Huang, W. F., Zeng, Q., Zhou, H., ... Huang, X. (2020). Evaluation of the exposure risk of SARS-CoV-2 in different hospital environment. *Sustainable Cities and Society*, 61, 102413. <https://doi.org/10.1016/j.scs.2020.102413>
- Ghini, I., McPherson, T. D., Hunter, J. C., Kirking, H. L., Christiansen, D., Joshi, K., ... Fricchione, M. J. (2020). First known person-to-person transmission of severe acute respiratory syndrome coronavirus 2 (SARS-CoV-2) in the USA. *The Lancet*. [https://doi.org/10.1016/S0140-6736\(20\)30607-3](https://doi.org/10.1016/S0140-6736(20)30607-3)
- Gilani, S., Montazeri, H., & Blocken, B. (2016). CFD simulation of stratified indoor environment in displacement ventilation: Validation and sensitivity analysis. *Building and Environment*, 95, 299–313. <https://doi.org/10.1016/j.buildenv.2015.09.010>
- Giordano, G., Blanchini, F., Bruno, R., Colaneri, P., Di Filippo, A., Di Matteo, A., ... Colaneri, M. (2020). Modelling the COVID-19 epidemic and implementation of population-wide interventions in Italy. *Nature Medicine*, 26(6), 855–860.
- Guo, Y., Qian, H., Sun, Z., Cao, J., Liu, F., Luo, X., ... Zhang, Y. (2021). Assessing and controlling infection risk with Wells-Riley model and spatial flow impact factor (SFIF). *Sustainable Cities and Society*, 67, 102719. <https://doi.org/10.1016/j.scs.2021.102719>
- Guo, Z. D., Wang, Z. Y., Zhang, S. F., Li, X., Li, L., Li, C., ... Zhang, M. Y. (2020). Aerosol and surface distribution of severe acute respiratory syndrome coronavirus 2 in hospital wards, Wuhan, China, 2020. *Emerging Infectious Diseases*, 26(7), 10–3201.
- Jin, T., Li, J., Yang, J., Li, J., Hong, F., Long, H., ... Luo, P. (2021). SARS-CoV-2 presented in the air of an intensive care unit (ICU). *Sustainable Cities and Society*, 65, 102446. <https://doi.org/10.1016/j.scs.2020.102446>
- Klepeis, N. E., Nelson, W. C., Ott, W. R., Robinson, J. P., Tsang, A. M., Switzer, P., ... Engelmann, W. H. (2001). The National Human Activity Pattern Survey (NHAPS): A resource for assessing exposure to environmental pollutants. *Journal of Exposure Science & Environmental Epidemiology*, 11(3), 231–252. <https://doi.org/10.1038/sj.jes.7500165>
- Kwon, S. B., Park, J., Jang, J., Cho, Y., Park, D. S., Kim, C., ... Jang, A. (2012). Study on the initial velocity distribution of exhaled air from coughing and speaking. *Chemosphere*, 87(11), 1260–1264. <https://doi.org/10.1016/j.chemosphere.2012.01.032>
- Lai, A. C., & Nazaroff, W. W. (2000). Modeling indoor particle deposition from turbulent flow onto smooth surfaces. *Journal of Aerosol Science*, 31(4), 463–476. [https://doi.org/10.1016/S0021-8502\(99\)00536-4](https://doi.org/10.1016/S0021-8502(99)00536-4)
- Li, X., Niu, J., & Gao, N. (2011). Spatial distribution of human respiratory droplet residuals and exposure risk for the co-occupant under different ventilation methods. *HVAC&R Research*, 17(4), 432–445. <https://doi.org/10.1080/1078969.2011.578699>
- Li, X., Niu, J., & Gao, N. (2013). Co-occupant's exposure to exhaled pollutants with two types of personalized ventilation strategies under mixing and displacement ventilation systems. *Indoor Air*, 23(2), 162–171. <https://doi.org/10.1111/ina.12005>
- Li, X., Yan, Y., Shang, Y., & Tu, J. (2015). An Eulerian–Eulerian model for particulate matter transport in indoor spaces. *Building and Environment*, 86, 191–202. <https://doi.org/10.1016/j.buildenv.2015.01.010>
- Li, Y., Huang, X., Yu, I. T. S., Wong, T. W., & Qian, H. (2005). Role of air distribution in SARS transmission during the largest nosocomial outbreak in Hong Kong. *Indoor Air*, 15(2), 83–95. <https://doi.org/10.1111/j.1600-0668.2004.00317.x>
- Li, Y., Leung, G. M., Tang, J. W., Yang, X., Chao, C. Y., Lin, J. Z., ... Sleigh, A. C. (2007). Role of ventilation in airborne transmission of infectious agents in the built environment-a multidisciplinary systematic review. *Indoor Air*, 17(1), 2–18. <https://doi.org/10.1111/j.1600-0668.2006.00445.x>
- Licina, D., Tian, Y., & Nazaroff, W. W. (2017). Inhalation intake fraction of particulate matter from localized indoor emissions. *Building and Environment*, 123, 14–22. <https://doi.org/10.1016/j.buildenv.2017.06.037>
- Liu, Y., Ning, Z., Chen, Y., Guo, M., Liu, Y., Gali, N. K., ... Liu, X. (2020). Aerodynamic characteristics and RNA concentration of SARS-CoV-2 aerosols in Wuhan hospitals during COVID-19 outbreak. *BioRxiv*. <https://doi.org/10.1101/2020.03.08.982637>
- Lu, J., Gu, J., Li, K., Xu, C., Su, W., Lai, Z., ... Yang, Z. (2020). COVID-19 outbreak associated with air conditioning in restaurant, Guangzhou, China, 2020. *Emerging Infectious Diseases*, 26(7), 1628. <https://doi.org/10.3201/eid2607.200764>
- Luo, L., Liu, D., Liao, X. L., Wu, X. B., Jing, Q. L., Zheng, J. Z., ... Liu, J. P. (2020). Modes of contact and risk of transmission in COVID-19: A prospective cohort study 4950 close contacts persons in Guangzhou of China. <https://doi.org/10.2139/ssrn.3566149>
- Melikov, A., & Kaczmarczyk, J. (2007). Measurement and prediction of indoor air quality using a breathing thermal manikin. *Indoor Air*, 17(1), 50–59. <https://doi.org/10.1111/j.1600-0668.2006.00451.x>
- Melikov, A. K., Bolashikov, Z. D., Kostadinov, K., Kierat, W., & Popiółek, Z. (2012). Exposure of health care workers and occupants to coughed air in a hospital room with displacement air distribution: Impact of ventilation rate and distance from coughing patient. *10th International Conference on Healthy Buildings*.
- Menter, F. R. (1994). Two-equation eddy-viscosity turbulence models for engineering applications. *AIAA Journal*, 32(8), 1598–1605. <https://doi.org/10.2514/3.12149>
- Morawska, L., & Cao, J. (2020). Airborne transmission of SARS-CoV-2: The world should face the reality. *Environment International*, 105730. <https://doi.org/10.1016/j.envint.2020.105730>
- Morawska, L., & Milton, D. K. (2020). It is time to address airborne transmission of coronavirus disease 2019 (COVID-19). *Clinical Infectious Diseases*, 71(9), 2311–2313. <https://doi.org/10.1093/cid/ciaa939>
- Morawska, L., Tang, J. W., Bahnhof, W., Bluyssen, P. M., Boerstra, A., Buonanno, G., ... Haworth, C. (2020). How can airborne transmission of COVID-19 indoors be minimised? *Environment International*, 142, 105832. <https://doi.org/10.1016/j.envint.2020.105832>

- Myatt, T. A., Johnston, S. L., Zuo, Z., Wand, M., Kebadze, T., Rudnick, S., ... Milton, D. K. (2004). Detection of airborne rhinovirus and its relation to outdoor air supply in office environments. *American Journal of Respiratory and Critical Care Medicine*, *169* (11), 1187–1190. <https://doi.org/10.1164/rccm.200306-760OC>
- Nazaroff, W. W. (2008). Inhalation intake fraction of pollutants from episodic indoor emissions. *Building and Environment*, *43*(3), 269–277. <https://doi.org/10.1016/j.buildenv.2006.03.021>
- Nazaroff, W. W., & Cass, G. R. (1986). Mathematical modeling of chemically reactive pollutants in indoor air. *Environmental Science & Technology*, *20*(9), 924–934.
- Nielsen, P. V., Li, Y., Buus, M., & Winther, F. V. (2010). Risk of cross-infection in a hospital ward with downward ventilation. *Building and Environment*, *45*(9), 2008–2014. <https://doi.org/10.1016/j.buildenv.2010.02.017>
- Noakes, C. J., Fletcher, L. A., Sleigh, P. A., Booth, W. B., Beato-Arribas, B., & Tomlinson, N. (2009). Comparison of tracer techniques for evaluating the behaviour of bioaerosols in hospital isolation rooms. *Proceedings of Healthy Buildings*, 13–17.
- Ong, S. W. X., Tan, Y. K., Chia, P. Y., Lee, T. H., Ng, O. T., Wong, M. S. Y., ... Marimuthu, K. (2020). Air, surface environmental, and personal protective equipment contamination by severe acute respiratory syndrome coronavirus 2 (SARS-CoV-2) from a symptomatic patient. *Jama*, *323*(16), 1610–1612. <https://doi.org/10.1001/jama.2020.3227>
- Pantelic, J., & Tham, K. W. (2013). Adequacy of air change rate as the sole indicator of an air distribution system's effectiveness to mitigate airborne infectious disease transmission caused by a cough release in the room with overhead mixing ventilation: A case study. *HVAC&R Research*, *19*(8), 947–961. <https://doi.org/10.1080/10789669.2013.842447>
- Pei, G., & Rim, D. (2021). Quality control of computational fluid dynamics (CFD) model of ozone reaction with human surface: Effects of mesh size and turbulence model. *Building and Environment*, *189*, 107513.
- Pei, G., Rim, D., Schiavon, S., & Vannucci, M. (2019). Effect of sensor position on the performance of CO2-based demand controlled ventilation. *Energy and Buildings*, *202*, 109358. <https://doi.org/10.1016/j.buildenv.2019.109358>
- Peric, M., & Ferguson, S. (2005). The advantage of polyhedral meshes. *Dynamics*, *24*(45), 504.
- Pung, R., Chiew, C. J., Young, B. E., Chin, S., Chen, M. I., Clapham, H. E., ... Low, M. (2020). Investigation of three clusters of COVID-19 in Singapore: Implications for surveillance and response measures. *The Lancet*. [https://doi.org/10.1016/S0140-6736\(20\)30528-6](https://doi.org/10.1016/S0140-6736(20)30528-6)
- Qian, H., Li, Y., Nielsen, P. V., Hyldgård, C. E., Wong, T. W., & Chwang, A. T. (2006). Dispersion of exhaled droplet nuclei in a two-bed hospital ward with three different ventilation systems. *Indoor air*, *16*(2), 111–128. <https://doi.org/10.1111/j.1600-0668.2005.00407.x>
- REHVA. (2020). COVID-19 guidance document. How to operate and use building services in order to prevent the spread of the coronavirus disease (COVID-19) virus (SARS-CoV-2) in workplaces. *Ventilation and air conditioning associations*. Federation of European Heating.
- Rim, D., & Novoselac, A. (2008). Transient simulation of airflow and pollutant dispersion under mixing flow and buoyancy driven flow regimes in residential buildings. *ASHRAE Transactions*, *114*, 130.
- Rim, D., & Novoselac, A. (2009). Transport of particulate and gaseous pollutants in the vicinity of a human body. *Building and Environment*, *44*(9), 1840–1849. <https://doi.org/10.1016/j.buildenv.2008.12.009>
- Rim, D., & Novoselac, A. (2010a). Occupational exposure to hazardous airborne pollutants: Effects of air mixing and source location. *Journal of Occupational and Environmental Hygiene*, *7*(12), 683–692. <https://doi.org/10.1080/15459624.2010.526894>
- Rim, D., & Novoselac, A. (2010b). Ventilation effectiveness as an indicator of occupant exposure to particles from indoor sources. *Building and Environment*, *45*(5), 1214–1224. <https://doi.org/10.1016/j.buildenv.2009.11.004>
- Rim, D., Novoselac, A., & Morrison, G. (2009). The influence of chemical interactions at the human surface on breathing zone levels of reactants and products. *Indoor Air*, *19* (4), 324. <https://doi.org/10.1111/j.1600-0668.2009.00595.x>
- Santarpia, J. L., Rivera, D. N., Herrera, V., Morwitzer, M. J., Creager, H., ... Santarpia, G. W., ... Lawler, J. V. (2020). Transmission potential of SARS-CoV-2 in viral shedding observed at the University of Nebraska Medical Center. *MedRxIV*. <https://doi.org/10.1101/2020.03.23.20039446>
- Setti, L., Passarini, F., De Gennaro, G., Barbieri, P., Perrone, M. G., Borelli, M., ... Miani, A. (2020). Airborne transmission route of COVID-19: Why 2 meters/6 feet of inter-personal distance could not be enough. <https://doi.org/10.3390/ijerph17082932>
- Shan, W., & Rim, D. (2018). Thermal and ventilation performance of combined passive chilled beam and displacement ventilation systems. *Energy and Buildings*, *158*, 466–475. <https://doi.org/10.1016/j.enbuild.2017.10.010>
- Sørensen, D. N., & Voigt, L. K. (2003). Modelling flow and heat transfer around a seated human body by computational fluid dynamics. *Building and Environment*, *38*(6), 753–762. [https://doi.org/10.1016/S0360-1323\(03\)00027-1](https://doi.org/10.1016/S0360-1323(03)00027-1)
- Somsen, G. A., van Rijn, C., Kooij, S., Bem, R. A., & Bonn, D. (2020). Small droplet aerosols in poorly ventilated spaces and SARS-CoV-2 transmission. *The Lancet Respiratory Medicine*. [https://doi.org/10.1016/S2213-2600\(20\)30245-9](https://doi.org/10.1016/S2213-2600(20)30245-9)
- Stadnytskyi, V., Bax, C. E., Bax, A., & Anfinrud, P. (2020). The airborne lifetime of small speech droplets and their potential importance in SARS-CoV-2 transmission. *Proceedings of the National Academy of Sciences*, *117*(22), 11875–11877. <https://doi.org/10.1073/pnas.2006874117>
- Sun, C., & Zhai, Z. (2020). The efficacy of social distance and ventilation effectiveness in preventing COVID-19 transmission. *Sustainable Cities and Society*, *62*, 102390. <https://doi.org/10.1016/j.scs.2020.102390>
- Tellier, R., Li, Y., Cowling, B. J., & Tang, J. W. (2019). Recognition of aerosol transmission of infectious agents: A commentary. *BMC Infectious Diseases*, *19*(1), 101. <https://doi.org/10.1186/s12879-019-3707-y>
- Van Doremale, N., Bushmaker, T., Morris, D. H., Holbrook, M. G., Gamble, A., Williamson, B. N., ... Lloyd-Smith, J. O. (2020). Aerosol and surface stability of SARS-CoV-2 as compared with SARS-CoV-1. *New England Journal of Medicine*, *382* (16), 1564–1567. <https://doi.org/10.1056/NEJMc2004973>
- Villafruela, J. M., Castro, F., San José, J. F., & Saint-Martin, J. (2013). Comparison of air change efficiency, contaminant removal effectiveness and infection risk as IAQ indices in isolation rooms. *Energy and Buildings*, *57*, 210–219. <https://doi.org/10.1016/j.enbuild.2012.10.053>
- WHO World Health Organization. (2020). *Transmission of SARS-CoV-2: Implications for infection prevention precautions: Scientific brief, 09 July 2020*. World Health Organization.
- Yan, W., Zhang, Y., Sun, Y., & Li, D. (2009). Experimental and CFD study of unsteady airborne pollutant transport within an aircraft cabin mock-up. *Building and Environment*, *44*(1), 34–43. <https://doi.org/10.1016/j.buildenv.2008.01.010>
- Yan, Y., Li, X., & Ito, K. (2020). Numerical investigation of indoor particulate contaminant transport using the Eulerian-Eulerian and Eulerian-Lagrangian two-phase flow models. *Experimental and Computational Multiphase Flow*, *2*(1), 31–40. <https://doi.org/10.1007/s42757-019-0016-z>
- Yin, Y., Gupta, J. K., Zhang, X., Liu, J., & Chen, Q. (2011). Distributions of respiratory contaminants from a patient with different postures and exhaling modes in a single-bed inpatient room. *Building and Environment*, *46*(1), 75–81. <https://doi.org/10.1016/j.enbuild.2010.07.003>
- Zhang, Z., Chen, X., Mazumdar, S., Zhang, T., & Chen, Q. (2009). Experimental and numerical investigation of airflow and contaminant transport in an airliner cabin mockup. *Building and Environment*, *44*(1), 85–94. <https://doi.org/10.1016/j.enbuild.2008.01.012>
- Zhu, S., Kato, S., & Yang, J. H. (2006). Study on transport characteristics of saliva droplets produced by coughing in a calm indoor environment. *Building and Environment*, *41*(12), 1691–1702. <https://doi.org/10.1016/j.enbuild.2005.06.024>